RANSAC-based DARCES: A New Approach to Fast Automatic Registration of Partially Overlapping Range Images

Chu-Song Chen, Yi-Ping Hung, Jen-Bo Cheng

Institute of Information Science, Academia Sinica, Nankang, Taipei, Taiwan

Email: hung@iis.sinica.edu.tw

Technical Report

Technical report, Institute of Information Science, Academia Sinica, TR-IIS-97-019, December 1997. A short version has been published on *Proceedings of International Conference on Computer Vision, ICCV'98*, Bombay, India, pp. 242-248, 1998.

Abstract

Many existing approaches used iterative-refinement techniques for 3D registration of partially-overlapping range images. The major drawback of these approaches is that they require a good initial estimate to guarantee that the correct solution can always be found. In this paper, we propose a new method, the RANSAC-based DARCES (data-aligned rigidity-constrained exhaustive search) method, which can solve the partially-overlapping 3D registration problem efficiently and reliably without any initial estimation. For the noiseless case, the basic algorithm of our DARCES method can guarantee that the solution it finds is the true one, due to its exhaustive-search nature. Even

with its exhaustive search nature, its time complexity can be shown to be relatively low. An extra characteristic is that our method requires no local features in the 3D data set.

1 Introduction

Registration of two partially-overlapping range images taken from different views is an important task in 3D computer vision. In general, if there is no initial knowledge about the poses of these two views, the information used in solving the 3D registration problem is mainly the 3D shape of the common parts of the two partially-overlapping data sets.

To make the discussion more rigorous, we give a formal definition of the 3D registration problem to be solved in this paper as follows:

Given two data sets: the model data set, $D_M = D_{M_O} \cup D_{M_U}$, and the scene data set, $D_S = D_{S_O} \cup D_{S_U}$, satisfying the following conditions:

1. The overlapping subsets of D_M and D_S can be denoted by $D_{M_O} = \{p_i = [x_i, y_i, z_i]^t \mid i = 1, 2, ..., n_o\}$ and $D_{S_O} = \{Rp_i + t + N_i \mid i = 1, 2, ..., n_o\}$, where R is a rotation matrix, t is a translation vector, N_i is a noise term and n_o is the number of data points contained in the overlapping subset, D_{M_O} or D_{S_O}. That is, D_{M_O} and D_{S_O} are two data sets which can be transformed so as to be exactly aligned for the *noiseless case* (i.e., $N_i = 0$) through the rigid-motion (R, t).

2. D_{M_O} is the unique largest possible overlapping region in D_M, whose *overlapping ratio*, i.e., $n_o/|D_M|$, is larger than a threshold Ω, where $|D_M|$ is the cardinality of D_M. Similarly, D_{S_O} is the unique largest possible overlapping region in D_S. The purpose of the assumption of this condition is to avoid meaningless solutions. Without this assumption, even the trivial case that two data sets overlap at a single point can be a legal solution.

The *3D registration problem* considered in this paper is to find the rigid-motion (R, t).

In the past, a popular type of approach to solving the 3D registration problem is the *iterative approach* [6][11]. Szeliski [26] has also proposed a method to register sparse range

data via a steepest-descent algorithm. The 3D registration problem can be formulated as a nonlinear parameter-estimation problem, and an iterative approach minimizes the error function iteratively if an initial estimate of the rigid-motion parameters is given in advance. Iterative approaches have the advantages that they are fast and easy-to-implement. However, the drawbacks are that (i) they require a good initial estimate to prevent the iterative process from being trapped in a local minimum, and (ii) there is no guarantee of getting the correct solution even for the noiseless case. Many approaches have modified the two approaches proposed in [6] and [11] to obtain more reliable correspondence in each iteration [13][14][15][21][28].

Another popular type of method is the *feature-based approach*. Feature-based approaches extract invariant local features first and then find the correspondences of features for estimation of the rigid transformation between two partially-overlapping 3D data sets. Stein and Medioni [25] proposed the splash structure, which is a local map describing the distributions of surface normals along a geodesic circle. Chua and Jarvis [12] used principle curvatures and Darboux frames to compute invariant features. Thirion [27] proposed a new type of feature, namely, *extremal points* of 3D surfaces. The features extracted using the above three approaches can be used for both 3D registration and recognition. Besides the use of point features, Gueziec [18] used *invariant curves* to find a partial match. Furthermore, some methods have also been proposed which extract feature primitives from structured-meshes for 3D registration [4][19]. Feature-based approaches have the advantage that they do not require initial estimates of the rigid-motion parameters. Their drawbacks are mainly that (i) they can not solve the problem in which the 3D data sets contain no prominent/salient local features, and (ii) a large percentage of the computation time is usually spent on preprocessing, which includes extraction of invariant features [12][25] and organization of the extracted feature-primitives (e.g., sorting [12], hashing[20] etc.). In addition, Blais and Levine expressed the 3D registration task as an optimization problem [7]. The very fast simulated reannealing (VFSR) technique was used to find the global minimum of the error function.

In practice, when the 3D data contained in two range images are to be registered, we

can treat one set as the *model data set* and the other as the *scene data set*, as we have formulated above. From this point of view, registration of two partially-overlapping 3D data sets is similar to the work of *3D object recognition* except that only one single object model is stored in the database for matching. Another difference is that object recognition may not require highly accurate alignment of the overlapping regions between the scene and the model data sets. That is, coarse alignment is usually sufficient for verification purposes in a recognition task. Hence, the methods which were developed for 3D object recognition can also be employed in solving the 3D registration problem in a coarse manner [2][10][23].

Preprocessing is an important technique which enables the 3D object recognition problem to be solved in an efficient way. This is because for a recognition task, multiple models are stored in a database. If some primitives or attributes are pre-extracted from each of the model-objects in an *off-line* process, the recognition speed can be greatly increased. For example, to deal with a recognition request, the scene data set is preprocessed only once, and the extracted primitives or attributes can then be used for matching each model stored in the database. If there are M models in the database, the matching time required for a recognition request is $t_p + Mt_m$, where t_p is the average time needed to pre-process the scene data set, M is the number of models contained in the database, and t_m is the average time required to match each model. If M is large, t_m dominates the computational speed for a complete recognition task. Hence, reduction of t_m is a major concern when building an efficient 3D object recognition system. On the other hand, the time required for a 3D registration task is $2t_p + t_m$ because preprocessing of both the model and the scene data sets must take place on line while the matching procedure only has to be performed once. Hence, if complex pre-processing for feature extraction is used, t_p may dominate the time required for the entire registration task. In fact, many existing feature-based methods for solving a 3D registration problem use a large percentage of the total time in preprocessing [5][12][25][27] [1]. Our goal in this paper is to solve the 3D registration problem in a fast and reliable

[1]For example, many feature-based methods took about 20-30 minutes to extract and organize useful feature-primitives, while the time required for finding the correspondences of features is less than one minute

manner. We propose a new method – the *data-aligned rigidity-constrained exhaustive search* (DARCES), which can check all possible data-alignments of two given 3D data sets in an efficient way while requiring no preprocessing and no initial estimates of the 3D rigid-motion parameters.

Furthermore, to solve the partially-overlapping 3D registration problem, the *random sample consensus* (RANSAC) scheme [17] is integrated into the DARCES procedure. We can prove that the proposed RANSAC-based DARCES approach can solve the partial matching problem of two 3D data sets with only a few random trials (see Section 3).

This paper is organized as follows. Section 2 introduces the DARCES method proposed in this paper. Section 3 presents the RANSAC-based DARCES approach. In Section 4, the RANSAC-based DARCES method is integrated into a coarse-to-fine structure to speed up 3D registration. Section 5 gives some experimental results. Finally, some discussion and conclusions are given in Sections 6 and 7, respectively.

2 Data-Aligned Rigidity-Constrained Exhaustive Search (DARCES)

Let two data sets, namely, the *scene data set* and the *model data set* be given. In this section, we will only consider a simpler 3D registration problem where the shape of the scene data set is *completely contained in* the shape of the model data set. We call such a problem the *fully contained 3D registration* (FC3DR) problem. After solving the FC3DR problem, the DARCES approach will be integrated into a RANSAC scheme [17] to solve the general partially-overlapping 3D registration problem.

[4][25][27].

2.1 Overview of The DARCES Algorithm

Let us treat the 3D data contained in a dense range image as a 3D surface. In the first place, we have to select some *reference points* from the scene surface, as shown in Fig. 1(a). For example, we can perform a uniform sampling from the indexing grids of the range images to select the reference points, or we can use all the data points contained in the scene data set as the reference points (but this will be less efficient). In the subsequent processing, a set of (at least three) *control points* is selected from these reference points, as shown in Fig. 1(b). The operation of the DARCES algorithm is somewhat like *sliding* of the control points (of the scene surface) on the model surface. During this sliding, all the selected reference points can be brought to some positions through a rigid-motion determined by these control points. In our approach, if the distance between a 3D reference point and the model surface is smaller than a threshold, then the point is regarded as being *successfully aligned* with the model surface. For each sliding position, we count the number of successfully aligned reference points. Finally, the rigid-motion associated with the sliding position which has the highest count is considered as the solution of our registration task. An overview of the DARCES algorithm is shown in the following.

[**Overview of the DARCES Algorithm**]
Given two 3D surfaces, the *model surface* and the *scene surface*. The shape of the scene surface is part of that of the model surface.

1. Select a set of *reference points* on the scene surface.

2. Select $k(k \geq 3)$ *control points* from these reference points.

3. For each rigid-transformation keeping all the control points lying on the model surface,
Do the following *verification steps* **3.1** and **3.2**.

3.1. Transform the reference points to new positions using the current rigid-transformation.

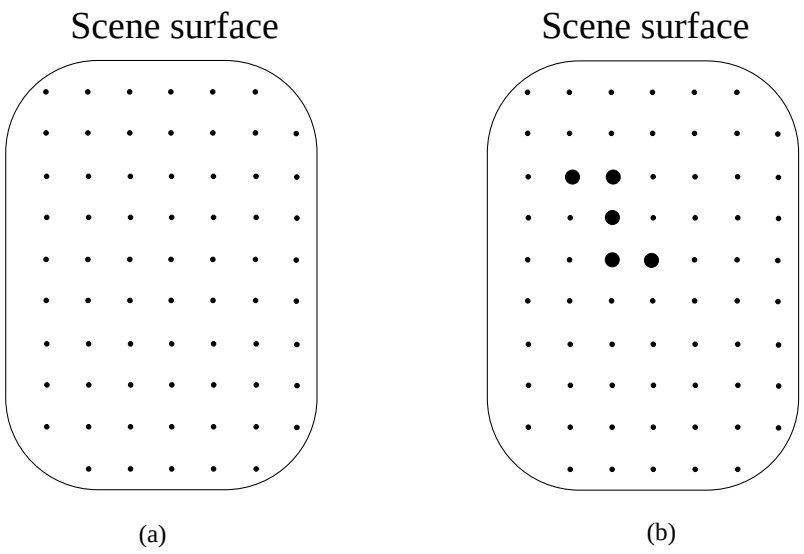

Figure 1: (a) Selection of the *reference points* in the scene surface. (b) Selection of a set of *control points* from these reference points.

3.2. Count the number of successfully aligned reference points. Assume the number is n_o.

4. Output the rigid-transformation with the largest number n_o.

A rigid-transformation has to be computed in the DARCES method when the control points move to new poses. Therefore, at least three control points are needed because the determination of a unique rigid-transformation requires at least three point correspondences. In this paper, given a set of point correspondences, the Arun, et al. method [3] is used to compute the LMS transformation of them.

Basically, $C_{n_c}^{n_s}$ combinations of control points can be selected, where n_s is the number of data points contained in the scene data set, and n_c is the number of the control points. However, it is not necessary to try all of these combinations. In fact, only one of them is sufficient to find the correct solution in the DARCES approach. How to choose an appropriate set of control points, and how many control points are required to solve the FC3DR problem will, respectively, be discussed in Sections 2.2.4 and 2.3.

2.2 Using Three Control Points

In this section, we will only consider the case where *three* control points are used. In the following, we call the three selected control points in the scene data set the *primary point* S_p, the *secondary point* S_s, and the *auxiliary point* S_a, respectively. The case in which more than three control points are used will be investigated in Section 2.3.

2.2.1 Search Range Reduction Using the Rigidity Constraints Generated by the Control Points

First, in the model data set, consider the possible corresponding positions of the primary point S_p. Without using feature attributes, every 3D point contained in the model data set can be the possible correspondence of the primary point. Hence, the primary point will be hypothesized as corresponding to each of the n_m points in the model data set, where n_m is the number of model points. [2]

Suppose S_p is hypothesized as corresponding to a model point M_p during the slide. Then, in the model data set, we will try to find some candidate points corresponding to the secondary point S_s. Assume that the distance between S_p and S_s is d_{ps}. The corresponding model point of S_s must lie on the surface of a sphere C_s whose center is M_p and radius is d_{ps}. That is, $C_s = \{\mathbf{p} = (x, y, z) \mid ||\mathbf{p} - M_p|| = d_{ps}\}$. In other words, once a corresponding model point of the primary point S_p is hypothesized, the search for M_s, the candidate model point corresponding to the secondary point S_s, can be limited to a small range, which is the surface of a sphere with radius d_{ps}, as shown in Fig. 2.

After a corresponding model point of the secondary point S_s has also been hypothesized, we can then consider the constrained search range of the auxiliary point S_a. Assume that S_p and S_s, respectively, now correspond to the model points M_p and M_s. The candidates of M_a, the corresponding model points of the auxiliary scene data point S_a, can be found within a limited search range determined by M_p, M_s and d_{qa}, where d_{qa} is the distance

[2] It is obvious that our method can be easily extended to use of some feature attributes associated with each 3D data point, e.g., 3D curvature or image luminance.

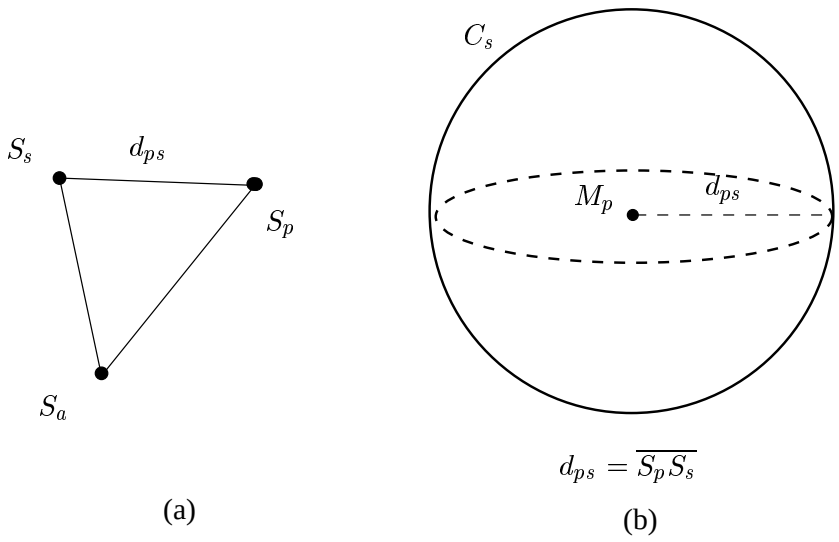

Figure 2: (a) The triangle formed by the three control points selected from the scene data set. (b) The search region of the secondary control point in the model data set is restricted to the surface of a sphere.

between S_q and S_a, and S_q is the orthogonal projection of S_a on to the line segment $\overline{S_p S_s}$, as shown in Fig. 3(a). It is easy to see that the candidates of M_a have to lie on the circle C_a centered at M_q with radius d_{qa}, where M_q is the 3D position corresponding to S_q. That is, $C_a = \{\mathbf{p} = (x, y, z) \mid ||\mathbf{p} - M_q|| = d_{qa}$, and $\overline{pM_q}$ is perpendicular to $\overline{M_p M_s}\}$.

After all the three control points are successfully aligned on the model surface, a unique rigid-transformation, namely T_c, can be determined by using the three point correspondence pairs: (S_p, M_p), (S_s, M_s) and (S_a, M_a). We then verify T_c by using all the reference points. With the rigid-transformation of T_c, all the reference points, $S_{r_1}, S_{r_2}, ..., S_{r_{n_r}}$, can be brought to new positions $S'_{r_1}, S'_{r_2}, ..., S'_{r_{n_r}}$. We count the number of occurrences, namely, N_o, when S'_{r_i} is successfully aligned on the model surface (i.e., the distance between S'_{r_i} and the model surface is smaller than a threshold) for all i, $i = 1, 2, ..., n_r$. Here, N_o is called the *overlapping number* of the transformation T_c, which is the LMS transformation determined by the three-point correspondence.

For each possible three-point correspondence, an overlapping number can be computed. Finally, the rigid-transformation with the largest overlapping number is selected as the so-

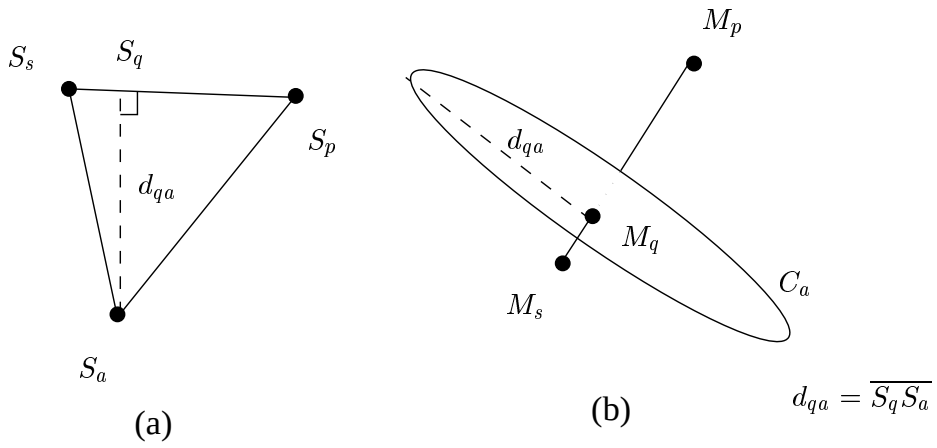

Figure 3: The search region of the auxiliary control point in the model data set is restricted to the contour of a 3D circle.

lution of our registration task. [3]

In general, the DARCES method can already provide the registration result accurate to some extent. However, standard fine-registration procedures [6][11] can be used for further refinement. In our method, an ICP-based method [28] is used to perform fine registration.

When the above strategy is used, the search ranges depend on the radii of the 3D sphere and 3D circle. In principle, the three control points form a triangle. Therefore, if a smaller triangle is employed when selecting the three control points, a faster search speed can be achieved. However, if the size of the triangle is too small, the computed rigid-transformation will be very sensitive to noise. Hence, determining an appropriate size for the above triangle is an important issue in our method. In Section 2.2.4, we will give a simple strategy for finding an acceptable minimal triangle for the DARCES algorithm.

[3] In general, there are no restrictions of the selections of the error measures in the DARCES method. In this paper, the largest number of matching points was chosen to be the error measure of accepting a match only because that it was easy to implement and also worked well in our experiments. Hence, different error measures, such as the weighted averages of the distances of the large-enough overlapping regions (as introduced in [7]), can be used as well.

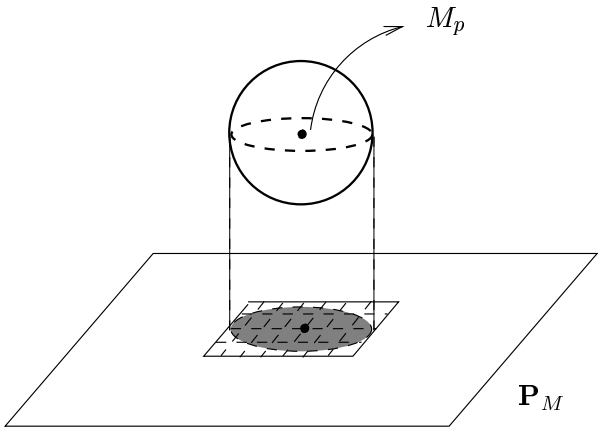

Figure 4: (a) The index plane of a set of 3D data points contained in a range image. (b)The 2D circular region of the projection of the 3D sphere onto the index plane; and the search of M_s is performed in a squared search region containing this circle.

2.2.2 Practical Implementation of the DARCES Method

For implementation purposes, direct searches in the 3D space on the surface of a sphere or on the boundary of a circle may not be trivial. To implement the DARCES approach efficiently, we exploit the fact that a range image can be treated as the projection of the 3D points onto an *index plane*. Assume that the index planes of the scene data set and the model data set are $\mathbf{P}_S$ and $\mathbf{P}_M$, respectively. To search M_s in the model data set, the 3D sphere C_s is projected onto $\mathbf{P}_M$ and, thus, forms a 2D circular region on $\mathbf{P}_M$, as shown in Fig. 4. To simplify the implementation, a square search region is used instead of a 2D circular region in our work. For each 3D point corresponding to the tessellation of the square search region, its distance to M_p is computed. Those 3D points whose distances are approximately d_{ps} are then recorded as the matching candidates of the second control point.

To search M_a, one method is to project the 3D circle C_a onto $\mathbf{P}_M$, thus forming a 2D ellipse on $\mathbf{P}_M$, as shown in Figure 5(a). The search can then be restricted to the 3D points corresponding to the boundary of the 2D ellipse on the indexing plane. However, indexing the boundary of a 2D ellipse is also not an easy task. In our approach, to make the implementation easier, we do not use the projection of the 3D circle C_a; instead, the projections

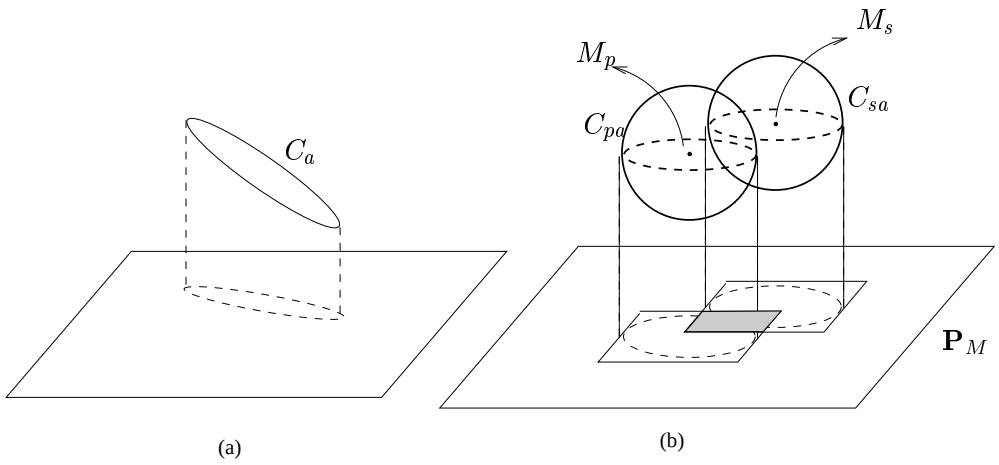

Figure 5: (a) The 2D ellipse of the projection of the 3D circle onto the index plane. (b) The search is performed in the intersection of the two squared regions.

of two other 3D spheres (C_{pa} and C_{sa}) are used, as shown in Fig. 5(b), where C_{pa} is the sphere whose center is M_p and whose radius is $\overline{S_p S_a}$, and C_{sa} is the sphere whose center is M_s and whose radius is $\overline{S_s S_a}$, respectively. The intersection of the two corresponding square regions of the two spheres C_{pa} and C_{sa} on the index plane is then used as the search region of the matching candidates of the auxiliary control point, as shown in Fig. 5(b).

To efficiently identify successful alignments, the index plane is also used to perform approximate estimation of the distance between a point and the model data set. Furthermore, verification can be speeded up using the following strategy: If the number of current accumulated votes is so small that even if all the remaining reference points are successfully aligned, the total number of votes will still be fewer than that of the largest one recorded, then the verification can be interrupted.

2.2.3 Complexity Analysis: the Case in which Three Control Points are Used

In the following, we will briefly analyze the computational complexity of the DARCES approach if three control points are used. The analysis result can then be used as an important guideline for the development of strategies used to speed up the DARCES method (see Section 2.2.4 and Section 4).

[DARCES algorithm using three control points]

1. Select three control points S_p, S_s, and S_a.

2. for($M_p \leftarrow$ each data point contained in the model data set) {

3. for($M_s \leftarrow$ each data point whose projection is contained in the projected region of the sphere C_s, in the index plane) {

4. if(the distance between M_s and M_p is approximate to d_{ps}) {

5 for($M_a \leftarrow$ each data point whose projection lies on the projected boundary of the 3D circle C_a, in the index plane) {

6. if(the distance between M_a and M_q is approximate to d_{qa}) {

7 compute the LMS rigid-transformation, namely, T_c, which transforms $\{S_p, S_s, S_a\}$ to $\{M_p, M_s, M_a\}$.

8 for($S_r \leftarrow$ each reference point contained in the scene data set, except S_p, S_s, and S_a) {

9 compute $M_r = T_c S_r$, if the distance between M_r and the model data set is smaller than a threshold, then M_r is labeled "successfully aligned".

}

10 $N_{T_c} \leftarrow$ the counts of the successful alignments (with respect to T_c).

}

}

}

}

}

11 output T_c with the largest counts N_{T_c}.

To simplify our derivation, assume that the distance, d, between the three selected control points is the same, i.e., they form a regular triangle as shown in Fig. 6. Since the first loop

(steps 3-10) will be executed n_m times (where n_m is the number of data points contained in the model data set), the time complexity will be $O(n_m \cdot T_1)$, where T_1 is the time required for a single iteration of the first loop (i.e., steps 3-10). Let n_d be the equivalent number of pixels (in the index plane) for an edge segment of length d. Steps 3 and 4 take $O({n_d}^2)$ because the surface of a sphere whose radius is d roughly contains ${n_d}^2$ points in the index plane. Steps 5-10 will be executed $O(n_d)$ times because only the data points contained in the intersection of the sphere C_s and the model surface will pass the "*if*" statement in step 4, and the intersection will typically be a 3D curve (or multiple 3D curves) containing roughly $O(n_d)$ points in the index plane. Hence, T_1 is equal to $O({n_d}^2 + n_d \cdot T_2)$, where T_2 is the time required for steps 5-10. Steps 5 and 6 take $O(n_d)$ because a circle whose radius is d roughly contains n_d points in the index plane. Steps 7-10 will be executed $O(1)$ times because the intersections of the sphere C_a and the model surface are typically two points (or more isolated points). Hence, T_2 is equal to $O(n_d + 1 \cdot T_3)$, where T_3 is the time needed for the verification steps (i.e., steps 7-10). Since verification takes $T_3 = O(n_r)$, the total time required for the DARCES method using three control points is $T^{\{S_p,S_s,S_a\}} = O(n_m({n_d}^2 + n_d(n_d + n_r))) = O(n_m \cdot {n_d}^2 + n_m \cdot n_d \cdot n_r)$.

According to the above analysis, the computation time of the DARCES method using three control points is dominated by three variables, n_m, d, and n_r. The smaller the three variables are, the faster is the DARCES method executed. Here, d (the edge length of the triangle) can be selected so as to increase the efficiency of the DARCES method. In the following, to choose an appropriate d, we will give an analysis of how to select an *acceptable minimal triangle* formed by the three control points. If the model data is too dense, n_m (the number of model data points) can also be reduced by re-sampling it so that the quantization error of the re-sampled data (i.e., the error along the X-Y direction) is approximately the average data acquisition error (i.e., the error along the Z direction). On the other hand, we will not investigate strategies for selecting n_r (the number of the reference points) because n_r is a dominant term *only for the case where three control points are used.* In fact, we will show that if more than three control points are used, then the computation speed will be

less sensitive to n_r.

2.2.4 Selection of the Acceptable Minimal Triangle

According to the complexity analysis, a smaller d will make the DARCES method more efficient. However, if d is too small, the induced rigid-transformation will be very sensitive to noise. In this section, we will try to find an acceptable minimal triangle to be used in the DARCES approach if three control points are used. In fact, the acceptable minimal size of the triangle can be theoretically derived if some of the parameters (e.g., the average data-acquisition error, and the error tolerance) are given in advance. Here, we also assume that the three selected control points form a regular triangle as shown in Fig. 6. Let the average position error of the data points (including both the data acquisition error of the range-finder and the quantization error) be e, and let c be the center of the triangle. Notice that the rigid-transformation T_c computed in our approach is based on the three point correspondences, (s_p, m_p), (s_s, m_s) and (s_a, m_a). However, the true positions of each model point m_p, m_s, and m_a are within spheres whose radii are e and centers are m_p, m_s, and m_a, respectively. Hence, for a scene point P whose distance to c is t, the alignment error caused by e will be enlarged to a x. Therefore, it can be easily found that x is $\sqrt{3}te/d$. Here, we define the *enlarge ratio* as $h = x/t$. If we want the enlarged ratio to be smaller than a threshold H, d should be larger than $d_{min} = \sqrt{3}e/H$, where d_{min} refers to the edge length of the acceptable minimal triangle. For example, assume that $e = 1.0$ millimeter (mm), and that we hope to keep the enlarge ratio smaller than $H = 0.1$. Then, $d_{min} = 17.32$ mm. In our work, the size of the triangle is fixed to a small constant, which is determined by means of the above-mentioned theoretical analysis. Thus, the time required for search can be significantly reduced.

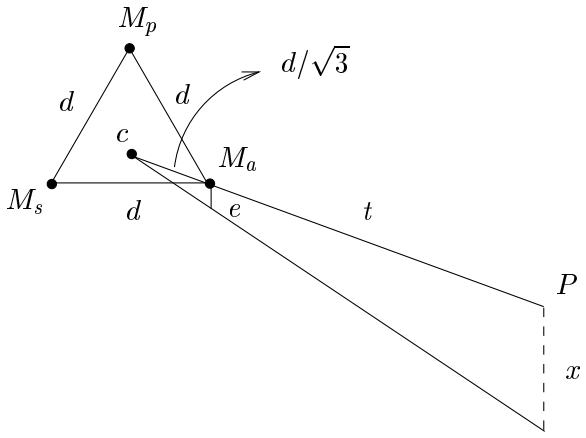

Figure 6: Derivation of the smallest triangle.

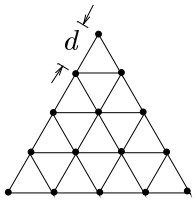

Figure 7: An example of selecting fifteen control points in the index plane.

2.3 Using More Than Three Control Points to Achieve More Efficient Search

We have clearly described and analyzed the DARCES algorithm when three control points are used. In this section, we will consider the case in which *more than three* control points are used. An interesting fact is that more efficient search can always be achieved in solving the FC3DR problem. Assume that n_c ($n_c > 3$) control points are selected from the scene data set, namely, the first three control points, S_p, S_s, S_a, and the other control points, S_4, S_5, ..., S_{n_c}, respectively. It should be noted that the first three control points, S_p, S_s, S_a, also have to be selected according to the principle that they form an acceptable minimal triangle. In our work, the other control points are usually selected such that their distances to their neighbors are approximately equal to the edge length of the triangle. For instance, Fig. 7 shows an example in which 15 control points are selected.

2.3.1 Search Range Reduction By Further Using the Rigidity Constraints

First we use the same search procedure introduced in the previous section to process the first three control points. Once the first three control points are successfully aligned to some model points, M_p, M_s and M_a, respectively, a rigid-transformation T_c can then be computed. Remember that the first constraint of the DARCES approach is to successfully align *all* of the control points on the model data set (see Section 2.1). To achieve this goal, we use T_c to sequentially transform each of the other control points S_i to new positions, $T_cS_4, T_cS_5, T_cS_6, ..., T_cS_{n_c}$. During the sequence of transformations, once there is a $T_cS_i, (i = 1, 2, ..., n_c)$ which violates the alignment constraint (i.e., its distance to the model data set is larger than a given threshold), then it is not necessary to try other transformations $T_cS_i, T_cS_{i+1}, ..., T_cS_{n_c}$ because we can directly assert that the current transformation T_c can not successfully align all the control points on the model data set. We call this speedup effect the *early jump-out* effect in this paper. Furthermore, in this case, it also is not necessary to further verify T_c by means of transformation of all the reference points, $S_{r_1}, S_{r_2}, ..., S_{r_i}$, to new positions. Therefore, the time required for verification can also be saved.

The number of control points n_c can be set to be any number between 3 and n_r. If we use more control points (i.e., a larger n_c), then the probability of "early jump-out" will be higher. Accordingly, in the noiseless case, the fastest way to solve the fully-contained 3D registration (FC3DR) problem is to *treat all the reference points as control points* in the DARCES procedure (i.e., choosing $n_c = n_r$). In this situation, once some control/reference points (except for the first three control points) can not be successfully aligned using the current transformation, transformations of all the other control/reference points can then be omitted.

Unfortunately, while the strategy of using as many control points as possible is better for solving the FC3DR problem, it is not always better for the partially-overlapping 3D registration problem. In principle, to solve the partially-overlapping 3D registration problem, it is required that all the control points lie in the overlapping region of the two data sets.

However, the more control points are used, the more likely it is that some of the control points will fall outside the overlapping region. Hence, it is an important issue to choose a good number of control points having good distribution. In general, determining the optimal number of control points is a difficult problem. This is because the optimal configuration of the control points depends on the size and the shape of the overlapping region of the two data sets (and thus, is quite data dependent). In our approach, we use a random-selection strategy to select of the control points, which will be introduced in Section 3.

2.3.2 Complexity Analysis: the Case in which More Than Three Control Points are Used

The algorithm of the DARCES method when more than three control points are used is similar to that in which only three are used, as introduced in Section 2.2.3, except for the following modifications:

1. Select n_c control points, including the first three, S_p, S_s, S_a and the others S_4, S_5,..., S_{n_c}.

7'. [a new step added between steps 7 and 8]

flag='success';

for(j=4; j$\leq n_c$, j++) {

if($M_j = T_c S_j$ is not successfully aligned on the model data set) {

flag='fail';

break; /* that is, break the above for loop */

}

}

if(flag='fail') {

continue; /* that is, continue the for loop in Step 5 */

}

8. for($S_r \leftarrow$ each reference point contained in the scene data set, except S_p, S_s, S_a, and S_4, S_5, ..., S_{n_c})

Exact complexity analysis of the case in which $n_c < n_r$ is difficult because different data

sets and different distributions of control points may result in different early jump-out effects. In general, if ς_1 and ς_2 are two selected sets of control points and T^{ς_1} and T^{ς_2} are their time complexities, respectively, then $\varsigma_1 \subset \varsigma_2$ implies that $T^{\varsigma 1_1} \leq T^{\varsigma_2}$. Therefore, a lower bound of the complexity can be derived if we consider the case where $n_c = n_r$. Basically, in this case, the verification steps (i.e., steps 8-10) will not be executed. Ideally, if early jump-outs always occur when dealing with the fourth control point, then the time complexity is $T^{all} = O(n_m \cdot {n_d}^2 + n_r)$ because only the correct solution can allow completion of the loop in step 7'. Hence, T^{all} is a lower bound of the complexity of the DARCES approach. In principle, if C is a set of control points in which the first three points are $\{S_p, S_s, S_a\}$, then $T^{all} \leq T^{\varsigma} \leq T^{\{S_p,S_s,S_a\}}$ (where $T^{\{S_p,S_s,S_a\}}$ has been derived in Section 2.2.3). It is worth noting that n_r (the number of reference points) is no longer a critical term in T^{all}. This implies an interesting fact that the more control points are used, the less influence n_r has on the time complexity. [4]

2.4 Discussion

From a theoretical point of view, the DARCES algorithm is an exhaustive-search method for solving the FC3DR problem. That is, all possible cases of successful alignment of two data sets are verified. Due to its exhaustive nature, the DARCES method has the following two advantages: (i) it can promise to obtain the correct solution for the noiseless case defined in Section 1, (ii) it can be applied even when the data sets have no prominent/salient local features, and (iii) it requires no initial estimate of rigid transformations.

On the other hand, the DARCES method is a highly-efficient exhaustive-search method. This is because that many useful constraints generated by the rigidity-relation of the data points are appropriately used including (i) the constrained search range of the possible corresponding positions of the second and the third control points (Section 2.2.1), (ii) the use of an acceptable minimal triangle (Section 2.2.4) for the first three control points, and (iii)

[4] However, the exact form of T^{ς} for $4 \leq n_c \leq n_r$ is difficult to be written as an analytical form, because it depends on the shape and the distributions of the data sets.

the use of more than three control points for the early jump-out of the verification process (Section 2.3). Compared to the optimization strategy proposed in [7], the DARCES method does not search in the parameter space without any constraints. Instead, it only searches the parameters which make the two data sets aligned.

The DARCES method can also be used in a flexible manner as discussed in the following. (1) If an initial estimate of the rigid-transformation is available, it can also be easily utilized in the DARCES approach. In principle, we can use it to restrict the search range of the primary control point. First, the scene data can be transformed in advance using the initial estimation of the rigid-transformation. Then, the search range of the primary control point can be restricted within a neighboring region.

(2) The DARCES method can be applied to either the original 3D data or the extracted feature data (e.g., the 3D points in the invariant curves [8][22]) contained in range images. That is, it can also be easily extended to use of some feature attributes associated with each 3D data point, e.g., 3D curvature or image luminance.

3 RANSAC-Based DARCES Approach for Partially-Overlapping Case

In the previous section, we have introduced the DARCES method for solving the FC3DR problem. In this section, to solve the general partially-overlapping 3D registration problem, we combine the DARCES method with a robust estimation method, the RANSAC scheme [17]. The RANSAC-based DARCES approach starts by randomly selecting a primary control point from the scene data set. Notice that only the primary control point S_p is selected randomly while the others are determined based on S_p and the length of the minimal triangle, d_{min}, as introduced in Section 2.3. Once the control points are selected, the DARCES procedure is performed to find possible alignments of these two data sets. If the rigid transformation found by the DARCES procedure has an overlapping number larger than a

threshold, then that transformation is regarded as the solution of our 3D registration task; otherwise, we select another primary point randomly from the scene data set and perform the above procedure again until it successfully finds a rigid transformation having a sufficiently large overlapping number.

The RANSAC-based DARCES algorithm is a modification of the DARCES scheme using more than three control points. Those modifications are:

1. The primary control point, S_p, is randomly selected. The other control points are then selected according to the principle that their distances to their neighbors are, approximately, d_{min}.

11. If the largest count of N_{T_c} is larger than a pre-given threshold Ω, then output T_c and stop; Else, goto 1;

Step 11 gives a *stopping rule* for the RANSAC-based DARCES algorithm. The threshold Ω is proportional to the allowed minimal overlapping ratio of the two partially-overlapping data sets, which has to be given in advance.

A statistical analysis of the required number of random trials is given below to show that our method can solve the partially-overlapping 3D registration problem with only a few random trials. First, consider the case where three control points are used. To simplify our analysis, we assume that the *overlapping region* (OR) in the index plane of the scene data set is a square region whose edge length is l as shown in Fig. 8. Suppose the shape and size of the triangle used in our approach is fixed; all of the three control points will lie in the overlapping region if the primary control point falls into the *eroded overlapping region* (EOR), as shown in Fig. 8. Assume that the number of data points contained in the OR of the scene data set is n_o. Then, $r = n_o/n_s$ is referred to as the *overlapping ratio* of OR, where n_s is the number of scene data points. From Fig. 8, the ratio of the area of the EOR to that of the OR can be shown to be $(l-d)^2/l^2$. Therefore, in a single random selection, the probability that the primary control point lies in the EOR is $p = r \cdot (l-d)^2/l^2$. Hence, the expected number of random trials is $E = 1 \cdot p + 2 \cdot (1-p)p + 3(1-p)^2 p + ... = 1/p$. Similar derivations can also be used for the case where more than three control points are

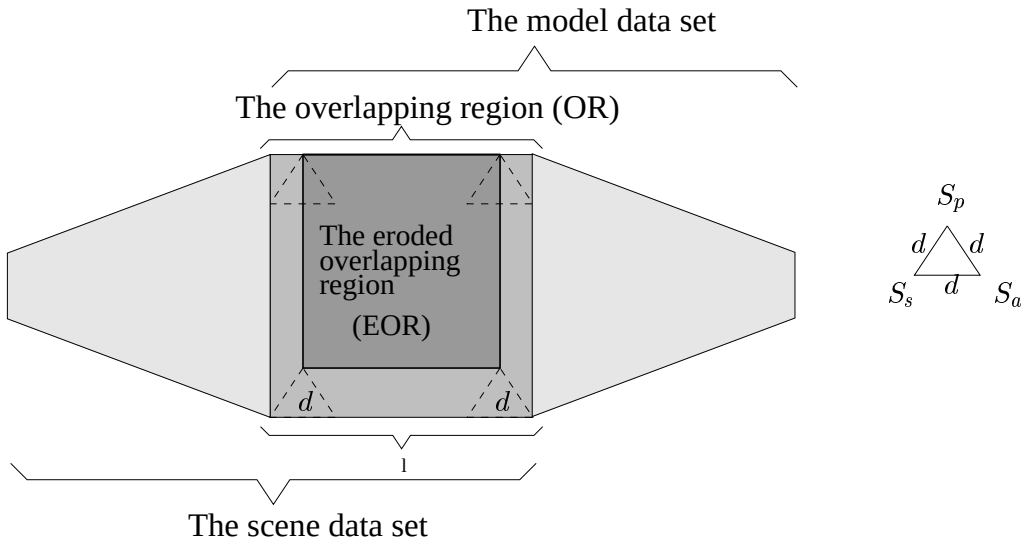

Figure 8: If the primary control point is set to lie in the eroded overlapping region, then all of the three control points will lie in the overlapping region.

used. For instance, consider the case where 15 control points are used. If the edge length of the triangle formed by the first three control points is 17.32 mm (which is the same as the one given in Section 2.2.4), then the edge length formed by the 15 control points is 69.28 mm (see Fig. 7). Assume that the edge length of the overlapping square is 120 mm, and that the overlapping ratio is 0.75. Then, the expected number of random trials is 7.46.

4 Coarse To Fine Scheme: Three-Step Algorithm

The RANSAC-based DARCES procedure described above is referred to as the *basic algorithm* of our approach. However, due to its exhaustive-search nature, the computation time is difficult to further reduce without using other constraints. Consequently, if we want to further speed up the DARCES method, the restriction of *exhaustive* search may have to be appropriately loosened. That is, by not requiring that all the possible alignments be searched, the speed can be considerably increased (hopefully, without affecting the outcome of the search in most cases). If no local features are used, the regularity of the data distribution will make it possible for the DARCES approach be easily incorporated into a coarse-to-fine

search structure. The speedup strategy we have adopted is the *three-step algorithm*, which is popular in the field of image/video coding [1]. The three-step algorithm is an n level coarse-to-fine method, where n is typically (but not restricted to be) three. In our approach, the three-step algorithm is used to further constrain the search ranges of the primary control point, S_p. First, the correspondences of S_p are searched on the grids of the coarsest level (i.e., level 1) in the index plane, as shown in Fig. 9. The best correspondence obtained from level 1 is then used as an initial estimate for the next level. In level 2, the search range for the possible correspondences of S_p can be restricted to a local region around the initial estimate obtained from level 1. Then, the best correspondence of S_p obtained in level 2 can be used as an initial estimate for searching the best correspondence of S_p in level 3. Notice that in the three-step algorithm, only S_p is searched in a coarse-to-fine manner. Once S_p is hypothesized to correspond to a model point, the correspondence candidates of all the other control points are searched in the finest level.

To make the combination of the RANSAC scheme and the three-step algorithm more efficient, a sequence of non-decreasing thresholds, Ω_1, Ω_2,...Ω_k, is, respectively, given in advance for the coarse to fine levels. [5] If the overlapping number computed at a coarser level is smaller than the threshold of this level, then we stop the search in the finer levels and immediately start another random trial.

5 Experimental Results

Figs. 10(a) and (b) show two range data sets of an object grabbed from two different view points. The range images were grabbed using a stereo range finder similar to that described in [9]. Their viewing angles differ by about 30^o. Each of them contains roughly 3650 data points. The RANSAC-based DARCES method was used to register the data sets contained in the two range images, which process was referred to as *coarse registration* in our

[5] In our experiments, four levels were used. The thresholds used for the coarsest and the finest levels were 0.1 and 0.65, respectively.

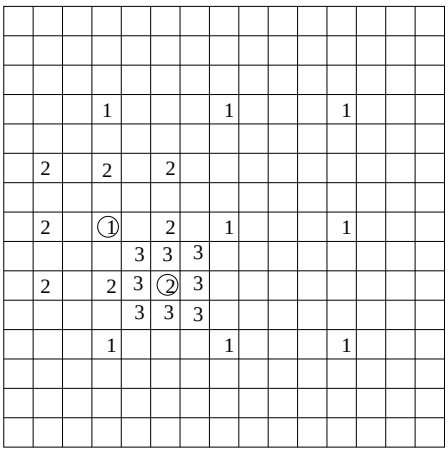

Figure 9: The three-step algorithm is used in the DARCES approach to find the corresponding positions of the primary control point in a coarse to fine manner.

experiment. The three-step algorithm was also used to further speed up the RANSAC-based DARCES approach. After that, a modified ICP approach [28] was used to refine the obtained 3D rigid-transformation, which was referred to as *fine registration* in our experiment. The average registration error of coarse registration was 3.74 millimeters (mm), and that of fine registration was 0.21 mm. In our experiment, 14 control points and 244 reference points were used. Two random trials were required to find the correct registration. The CPU time needed for registration was 5.85 seconds, where coarse registration took 5.03 seconds and fine registration took 0.82 seconds (using a SGI O^2 workstation). Notice that the computation time was measured for the entire 3D registration task, instead of treating some procedures as off-line processes (such as the feature-extraction procedure and the feature-organization procedure in a feature-based approach). After performing the 3D registration task, a 3D rigid transformation $T = (R, t)$ was computed. Figs. 10(c) and (d) show the transformations of the meshes of Figs. 10(a) and (b) using T_{mid} and T_{mid}^{-1}, respectively, where $T_{mid} = \sqrt{T}$. The set of randomly selected control points which led to successful registration is shown in Fig. 10(e). Figs. 10(f) shows the direct overlap of the two data sets observed from the middle view, and Fig. 10(g) shows the integrated triangle mesh of the two overlapping data sets. [6]

[6] We implemented the zippering method [28] to integrate the two overlapping range data sets.

Another example is shown in Fig. 11. Fig. 11(a) consists of nine range images of a toy obtained from different view points. Each range image contained about 6000 3D data points. Their viewing angles also differed by about 30^o. They were indexed as I_1, I_2,...,I_9. To register these nine range images, they were organized as a set of eight pairs of adjacent data sets, (I_1, I_2), (I_2, I_3),..., (I_8, I_9). [7] The intensity images are also obtained from the same view points as those used to obtain the range images, as shown in Fig. 11(b). Then, these range images were registered using the method described in this paper. Registration of each pair took on average 3.33 random trials, and the average CPU time needed to register each pair was 13.25 seconds (11.50 seconds for coarse registration and 1.75 seconds for fine registration). The average registration errors in this experiment were 1.61 mm for coarse registration and 0.84 mm for fine registration. As an example, the set of the randomly selected control points which led to successful registration for (I_5, I_6) is shown in Fig. 11(c). Once registered, these range images were transformed and integrated into a single data set. Then, by mapping and blending the intensity images onto the integrated data set, the texture-mapped images from three different selected views could be obtained and are shown in Figs. 11(d), (e), and (f).

Remember that in Section 2.3.2, we derived that the required computation time is not sensitive to the number of the reference points selected from the scene data set. To verify this property, we used different numbers of reference points to register the pair, (I_5, I_6). It can be observed from Table 1 that the execution time required for registration of the two data sets varied slowly from the case of using more reference points to that of using fewer. Hence, the experimental results coincide very well with the property that the number of reference points is not a critical term for the computational complexity. Amazingly, the successful registration could be achieved even when quite a few reference point were used

[7] In this experiment, we only registered these eight pairs and then integrated them as a single data set. The registration of the pair of the first and the last data sets, i. e., (I_9, I_1), was not considered here. If one wants to register them with a further constraint that I_1 and I_9 also have to be stitched, the registration result of this experiment can serve as a good initial estimate of a *global registration* method [4], which can be used for further global refinement.

in this case, which reveals that if the number of control points is far more than three, the spread of the control points may already carry sufficient shape information for the partial matching of the two data sets. In general, an appropriate large number of reference points is preferable because using more reference points can allow more accurate error estimation in the verification stage. [8]

Fig. 12(a) shows four range data sets of a model head obtained from different view points. Their viewing angles differ by about 45^o. Each of them contains roughly 4200 data points. The registered and integrated 3D data set is shown in Fig. 12(c). Figs. 12(d) and (e) show the shaded and the texture-mapped images of Fig. 12(c), respectively. The CPU time of total registration of the three pairs formed by the four data sets was 71.61 seconds, and the average registration error was 1.45 mm. In this experiment, the major amount of time was spent on registration of the first pair (55.72 seconds) because it took 20 random trials before good transformation was obtained. This is a good example showing the speedup effect of using a sequence of non-decreasing thresholds for the coarse to fine levels in combination with the RANSAC scheme and the three-step algorithm (as described in Section 4). In fact, if the threshold values used were set to be 0.65 for all levels, then the execution time for registration of the first pair could be increased to 170.39 seconds, which was more than triple the amount of time (i. e., 55.72 seconds) needed using 0.65 for the finest level and 0.1 for all the other coarser levels. Hence, using a sequence of thresholds can make the combination of the RANSAC scheme and the three-step algorithm more efficient (especially for cases which require more random trials).

In Figs. 13 (a) and (b), range images of a pair of fruits are shown from two different views. Fig. 13 (a) is the right view and Fig. 13 (b) is the left view. Their viewing angles differ by about 30^o. Each image contains roughly 2400 data points. Notice that in this case, the two range data sets contain no good local features. Hence, in general, it is difficult to

[8] In the implementation, we simply chose an appropriate sampling ratio (e. g., 4 by 4) for selection of several reference points by means of uniform sampling, and the number of control points selected in this way was usually several hundred in our experiments.

Table 1: The cpu time needed for coarse registration of (I_5, I_6) versus the number of reference points used ('F' denotes "fail to be registered").

n_r	5797	1461	666	375	246	173	130	73	42	28	20
seconds	8.59	5.28	4.54	4.34	4.28	4.23	4.15	4.13	4.08	4.07	F

solve this 3D registration problem if we use a feature-based method. Nevertheless, using the RANSAC-based DARCES approach, the two data sets can be successfully registered. Fig. 13 (c) shows the registered data set which needed only 3.95 seconds with two random trials.

6 Discussion

While our experimental results are encouraging, a limitation of the DARCES approach is that it is not appropriate for dealing with the 3D registration problem if either the 3D data is too noisy or the overlapping ratio is too small. To use the DARCES approach for 3D registration, the edge of the accepted minimal triangle, d_{min} (defined in Section 2.2.4) should be smaller than the width of the overlapping region, l (defined in Section 3), which yields $e/l < H/\sqrt{3}$ (because $d_{min} = \sqrt{3}e/H$, see Section 2.2.4). Let the average width of the data set be w; then, the overlapping ratio can be represented as $r = l^2/w^2$. Therefore, the relation holds for $r > \frac{3}{w^2H^2}e^2$. By combining the constraint that $r < 1$, a region delimited by a parabola curve and the horizontal line, $r = 1$, can be obtained, as shown in Fig. 14. Hence, to use the DARCES approach for 3D registration, (e, r) have to be within this region. It can be observed from Fig. 14 that (i) e has to be smaller than $WH/\sqrt{3}$, and (ii) the larger e is, the larger should be the overlapping ratio r. For example, if w is 160 mm and $H = 0.1$, then e should be smaller than 9.24 mm. If the overlapping ratio is 0.75, then the DARCES approach can be used if $e < 6.93$ mm. In practice, to avoid spurious solutions, it is reasonable to assume that the overlapping ratio of the two data sets should be large enough. Furthermore, due to progress in range data acquisition techniques, it is not difficult

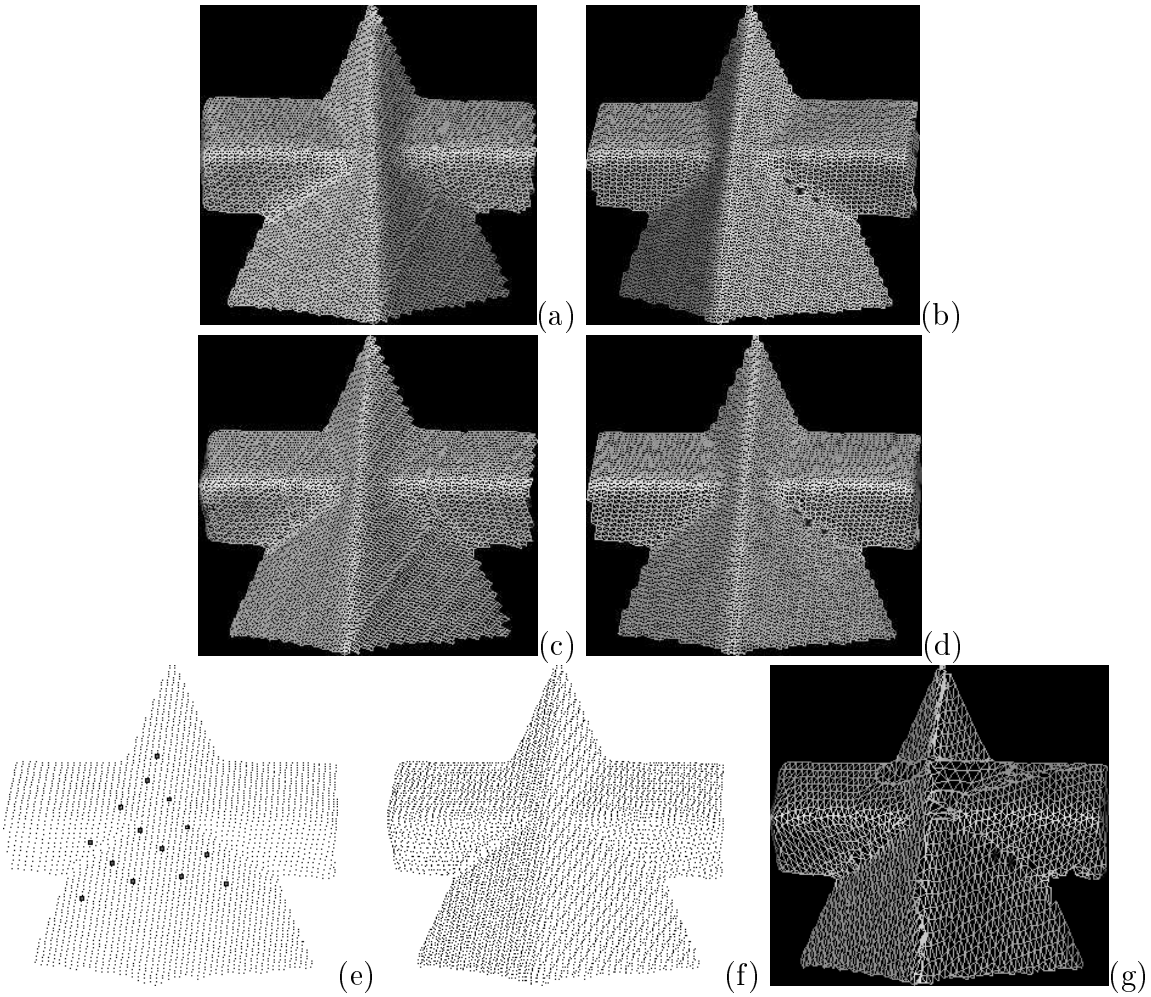

Figure 10: (a) and (b) show two dense triangular meshes of the range data of an object taken from two different view points. After performing the 3D registration task, a 3D rigid transformation $T = (R, t)$ was computed. (c) and (d) show the transformations of the meshes of (a) and (b) using T_{mid} and T_{mid}^{-1}, respectively, where $T_{mid} = \sqrt{T}$. (e) shows the set of randomly selected control points which led to successful registration (that is, those randomly selected in the last iteration). (f) shows the direct overlap of the two data sets observed from the middle view. (g) shows the triangular mesh obtained by integrating the two overlapping 3D data sets using the zippering method [28].

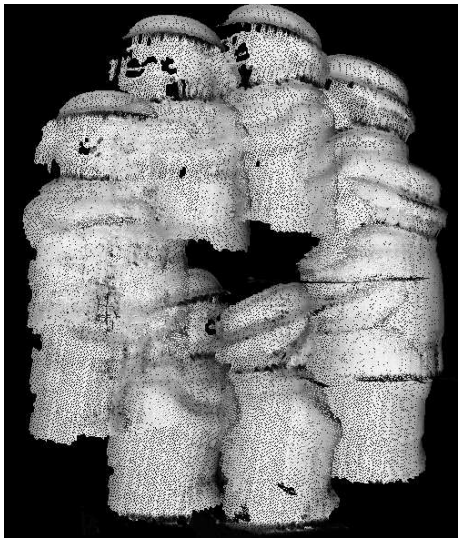

(a)

(b)

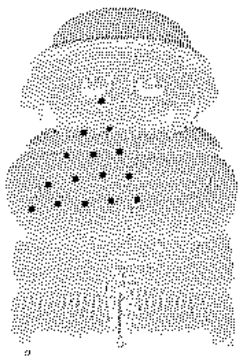

(c)

(d)

(e)

(f)

Figure 11: (a) shows nine range data sets of a toy grabbed from different view points. (b) shows the intensity images from the nine different view points where their range data are grabbed. (c) shows the set of randomly selected control points which led to successful registration for (I_5, I_6). Then, after performing 3D registration and by mapping and blending the intensity images onto the registered and integrated 3D data sets, the resulting texture-mapped images from three selected views were shown in (d),(e), and (f).

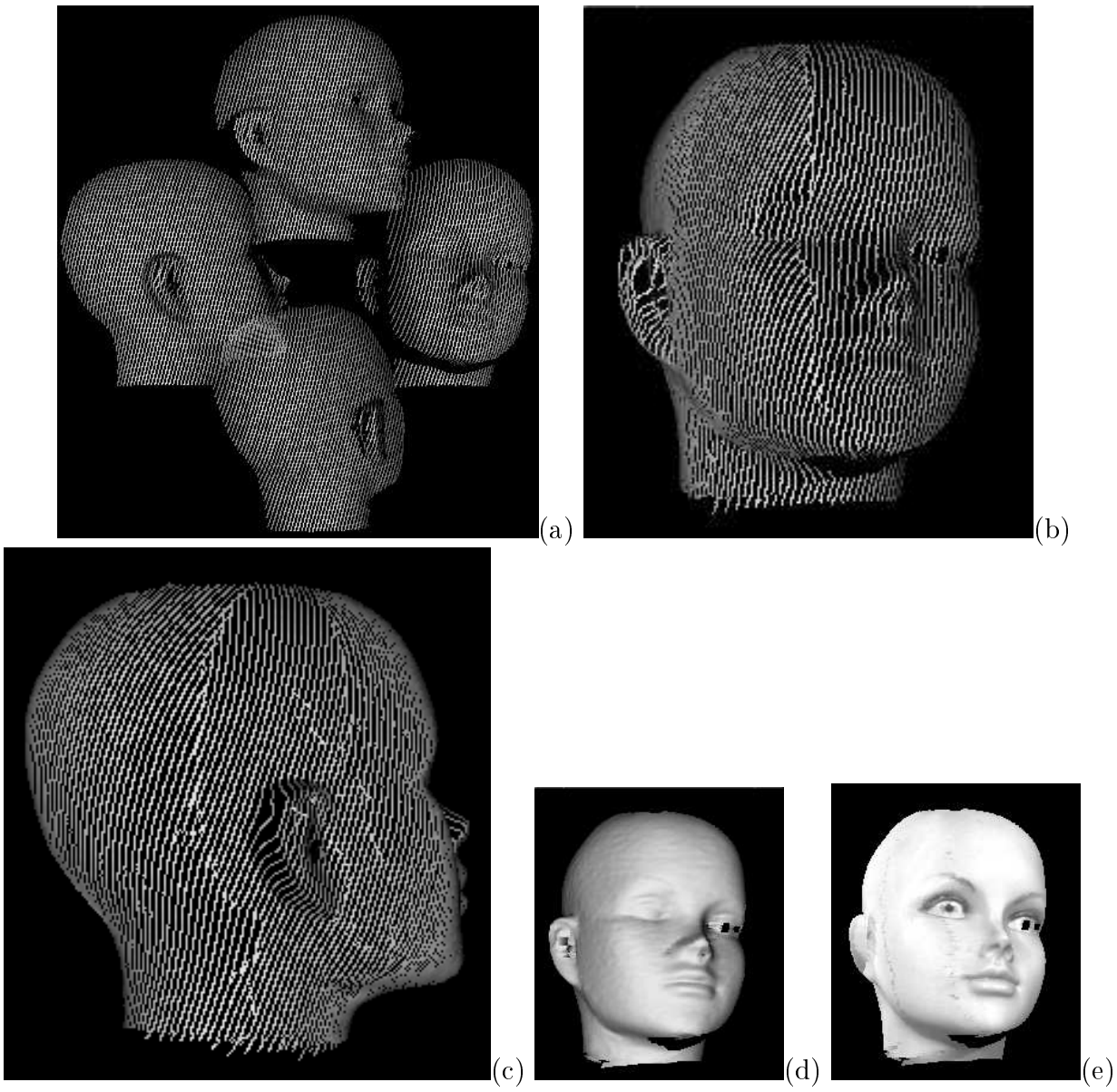

Figure 12: (a) shows four range images grabbed from different view points. (b) and (c) are the results of registration and integration, observed from two different viewing directions. (d) is the shaded image of the integrated 3D data set. (e) The texture mapped image of the integrated 3D data set.

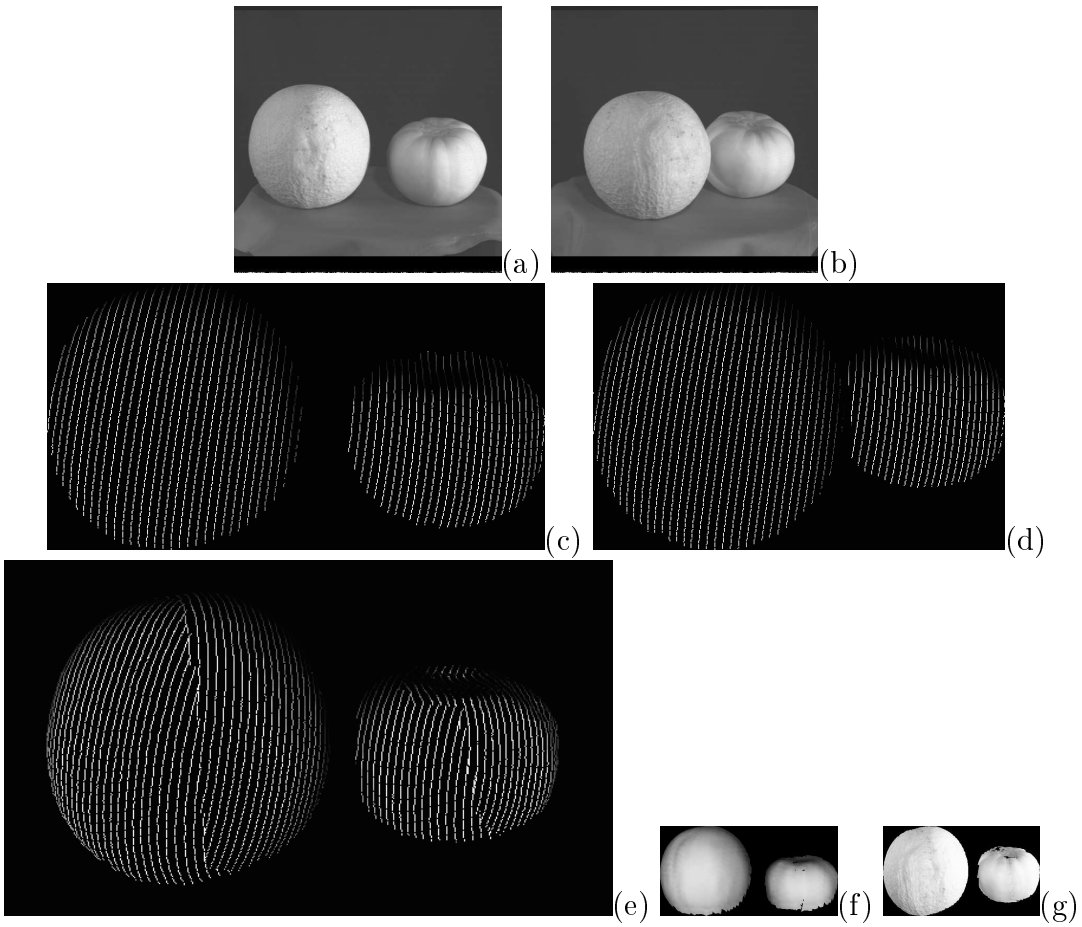

Figure 13: (a) and (b) are a pair of fruits observed from different view points. (c) and (d) show their range data. The two data sets contain almost no local features and, hence, are difficult to register using a feature-based approach. (e) shows the 3D data set registered using the RANSAC-based DARCES approach. (f) is the shaded image of the integrated 3D data set. (g) The texture mapped image of the integrated 3D data set.

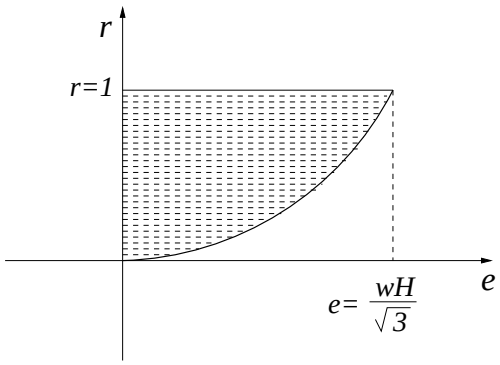

Figure 14: The (e, r) region in which the DARCES approach can be used, where e is the average data acquisition error, and r is the overlapping ratio.

to develop a range finder whose data acquisition error is within the range of 50 microns to 1.0 mm by using well-calibrated visual sensors. Hence, the DARCES approach can always be applied to most practical cases.

Although the RANSAC-based DARCES approach is designed to solve the 3D registration problem, it also has great potential for application in general 3D object recognition (perhaps through a combination of some appropriate curve-based feature-extractions). We plan to investigate this problem in the future.

7 Conclusions

Most of the existing techniques for solving the partially-overlapping 3D registration problem have one of the following limitations:

1. They can not ensure a correct solution even for the noiseless case [6][14][11][28].
2. They require a good initial estimate of the rigid transformation between the two data sets [6][11].
3. They can only be used if the data sets contain sufficient local features [12][18][25].

In this paper, we have proposed the RANSAC-based DARCES approach, which has none of the above three limitations. The basic algorithm of our approach can guarantee that the solution it finds is the true one, and it can be used for the featureless case while requiring

no initial estimates. Also, our method is faster than most of the existing methods which do not require initial estimations. Our approach simply treats the 3D registration problem as a partial-matching problem and uses the rigidity constraint among some pre-selected control points to restrict the search range used for matching. Although some approaches have also used rigidity constraints to facilitate the matching processes [12][14][27], our approach is the first one to show that the 3D registration problem can be solved in a relatively low-order computation time by carefully using all of the constraints provided by the rigidity. In addition, we have indicated that by appropriately selecting the number and the distribution of the control points, the computation time can be greatly reduced. Therefore, we have shown how the acceptable minimal triangle formed by the first three control points can be determined, and how additional control points can be used to speed up the search process. Finally, we have integrated into our method the three-step algorithm and shown that the computation time can be further reduced while keeping the registration reliable with the help of the RANSAC scheme. Although the principle used in our approach is simple and easy-to-implement, to the best knowledge of the authors, no one has adopted similar ideas to solve the 3D registration problem. Experiments have demonstrated that our method is efficient and reliable for registering partially-overlapping range images.

References

[1] *MPEG standard draft ISO-IEC/JTC1 SC29 on 22*, November, 1991.

[2] F. Arman and J. K. Aggarwal, "Model-Based Object Recognition in Dense-Range Images – A Review,", *ACM Computing Survey*, Vol. 25, No. 1, pp. 125-145, 1993.

[3] K. S. Arun, et. al, "Least-Square Fitting of Two 3-D Point Set," *IEEE Trans. PAMI*, Vol. 9, pp. 698-700, 1987.

[4] R. Bergevin, et. al, "Towards a General Multi-View Registration Technique," *IEEE Trans. PAMI*, Vol. 18, No. 5, pp. 540-547, 1996.

[5] R. Bergevin, et. al, "Registering Range Views of Multipart Objects," *Computer Vision and Image Understanding*, Vol. 61, No. 1, pp. 1-16, 1995.

[6] P. J. Besl and N. D. McKay, "A Method for Registration of 3-D Shapes," *IEEE Trans. PAMI*, Vol. 14, pp. 239-256, 1992.

[7] G. Blais and M. D. Levine, "Registering Multiview Range Data to Create 3D Computer Objects," *IEEE Trans. PAMI*, Vol. 17, No. 8, pp. 820-824, 1995.

[8] C. S. Chen, et. al, "Extraction of Corner-Edge-Surface Structure from Range Images Using Mathematical Morphology," *IEICE Trans. Information and Systems*, Vol. E78-D, Special Issue on Machine Vision Applications, pp. 1636-1641, 1995.

[9] C. S. Chen, et. al, "Range Data Acquisition Using Color Structured Lighting and Stereo Vision," *Image and Vision Computing*, Vol. 15, pp. 445-456, 1997.

[10] C. S. Chen, et. al, "Model-Based Object Recognition with Range Images by Combining Morphological Feature Extraction and Geometric Hashing," *Proc. 13th International Conference on Pattern Recognition*, Vienna, Austria, pp. 565-569, 1996.

[11] Y. Chen and G. Medioni, "Object Modeling by Registration of Multiple Range Images," *Image and Vision Computing*, Vol. 10, No. 3, pp. 145-155, 1992.

[12] C. S. Chua, "3D Free-Form Surface Registration and Object Recognition", *International Journal of Computer Vision*, 17, pp. 77-99, 1996.

[13] C. Dorai, et. al, "From Images to Models: Automatic 3D Object Model Construction from Multiple Views," *Proc. International Conference on Pattern Recognition Vol. 1*, pp. 770-774, 1996.

[14] C. Dorai, J. Weng, A. K. Jain, and C. Mercer, "Registration and Integration of Multiple Object Views for 3D Model Construction," *IEEE. Trans. PAMI*, pp. 83-89, 1998.

[15] D. Eggert, et. al, "Simultaneous Registration of Multiple Range Views for Use in Reverse Engineering," *Proc. International Conference on Pattern Recognition*, Vienna, Austria, pp. 243-247, 1996.

[16] O. Faugeras, *Three-Dimensional Computer Vision*, The MIT Press, London, England, 1993.

[17] M. A. Fischler and R. C. Bolles, "Random Sample Consensus, A Paradigm for Model Fitting with Applications to Image Analysis and Automated Cartography," *Communications of the ACM*, Vol. 24, No. 6, pp. 381-395, 1981.

[18] A. Gueziec and N. Ayache, "Smoothing and Matching of 3D Space Curves," *International Journal of Computer Vision*, 12:1, pp. 79-104, 1994.

[19] K. Higuchi, M. Hebert, and K. Ikeuchi, "Building 3-D Models from Unregistered Range Images," *Graphical Models and Image Processing*, Vol. 57, No. 4, pp. 315-333, 1995.

[20] Y. Lamdan, et. al, "Affine Invariant Model-Based Object Recognition," *IEEE Trans. Robotics and Automation*, Vol. 6, pp. 578-589, 1990.

[21] T. Masuda and N. Yokoya, "A robust Method for Registration and Segmentation of Multiple Range Images," *Computer Vision and Image Understanding*, Vol. 61, pp. 295-307, 1995.

[22] O. Monga, et. al, "Using Partial Derivatives of 3D Images to Extract Typical Surface Features," *Proc. International Conference on Computer Vision and Pattern Recognition*, Urbana Champaign, IL, 1992.

[23] M. Suk and S. M. Bhandarkar, *Three-Dimensional Object Recognition from Range Images*, Springer Verlag, 1992.

[24] M. Soucy and D. Laurendeau, "A General Surface Approach to the Integration of a Set of Range Views," *IEEE Trans. PAMI*, Vol. 17, pp. 344-358, 1995.

[25] F. Stein and G. Medioni, "Structural Indexing: Efficient 3-D Object Recognition," *IEEE Trans. PAMI*, Vol. 14, No. 2, pp. 125-145, 1992.

[26] R. Szeliski, "Estimating Motion from Sparse Range Data Without Correspondence," Proc. Second International Conference on Computer Vision, pp. 207-216, 1988.

[27] J. P. Thirion, "New Feature Points Based on Geometric Invariants for 3D Image Registration," *International Journal of Computer Vision*, 18(2), pp. 121-137, 1996.

[28] G. Turk and M. Levoy, "Zippered polygon Meshes from Range Images," *Proc. SIGGRAPH*, pp. 311-318, 1994.